

# ROBUST WIND POWER CONTROL USING SLIDING MODE, BACKSTEPPING, AND FUZZY LOGIC

ABDELGHAFOR HERIZI<sup>1</sup>, RIYADH ROUABHI<sup>2</sup>, FAYSSAL OUAGUENI<sup>3</sup>, ABDERRAHIM ZEMMIT<sup>4</sup>

**Keywords:** Doubly fed induction generator; Sliding mode control; Backstepping control; Fuzzy logic; Hybrid; Power control.

This paper presents a novel nonlinear control approach for a doubly fed induction generator (DFIG) by integrating sliding mode control, backstepping control, and fuzzy logic. The proposed hybrid strategy modifies the sliding mode controller by retaining the equivalent control while replacing the attractive control with backstepping. Type-1 fuzzy logic is then used to optimize the stabilization gains of the backstepping controller, enhancing system stability and resilience. The effectiveness of the proposed control is evaluated through MATLAB/Simulink simulations. Results from the tracking test show accurate reference trajectory tracking without exceeding active and reactive power limits or exhibiting steady-state errors. In the regulation test, the system demonstrated sensitivity to sudden speed changes but maintained stable active and reactive power.

## 1. INTRODUCTION

In recent years, growing global awareness of sustainable energy sources and a reduced dependence on fossil fuels has led to an increasing interest in renewable energy technologies, particularly wind power, which is one of the most promising and rapidly growing sectors. Wind power, a clean and abundant source of energy, has prompted numerous research and development initiatives worldwide.

The variable-speed wind turbine utilizing a doubly fed induction machine is the most popular due to its high energy efficiency and controllability [1]. The stator windings of the DFIM, operating in generator mode, are connected directly to the power grid. In contrast, the rotor windings are connected to a power converter via sliding contacts (brush rings). To extract and supply optimum power to the power grid, the rotation speed of the generator must be controlled through this power converter by adjusting the rotor frequency. Here, the range of the rotation speed is 30% (or 33%) around the synchronous speed [2]. Additionally, this converter is sized to handle only 20-30% of the machine's nominal power. This makes this type of wind system economically attractive [3]. Doubly fed induction generators (DFIGs) are commonly employed in contemporary wind turbines because they provide an efficient capture of wind energy and enable more effective control of power quality and grid stability [4, 5].

However, despite their many advantages, wind energy conversion systems based on DFIGs face challenges related to control strategies, especially in scenarios where the system operates under variable wind conditions and is subject to disturbances [6]. To address these challenges, advanced control techniques have been studied to improve the performance and stability of DFIG systems. We can distinguish in a non-exhaustive way the sliding mode control, which took off in the late seventies when "Utkin" introduced the sliding mode theory [1, 7-10], and the backstepping control [11-14].

On the other hand, a significant development has occurred over the last two decades. In fact, the emergence of new techniques, such as fuzzy logic, neural networks, and genetic algorithms, has enabled the development of a new discipline known as artificial intelligence. Artificial intelligence techniques have allowed, not only to improve the control of systems and to overcome the disadvantages of classical techniques.

Fuzzy logic represents a significant subfield of artificial

intelligence. The theoretical foundations of this logic were established in 1965 by Professor Lotfi Zadeh at the University of California, Berkeley, who introduced the concept of the fuzzy set [15, 16]. This enables the generation of a control law that is frequently highly effective without the necessity for comprehensive modelling. In contrast to a conventional regulator or a state feedback regulator, a fuzzy logic regulator does not process a clearly defined mathematical relationship. Instead, it employs inferences based on multiple rules and linguistic variables. It is thus possible to take into account the experiences acquired by operators of a technical process. Fuzzy logic is a highly effective method for enhancing the resilience of control systems to parametric and non-parametric variations [1, 7, 12, 17-19].

In this study, a robust control system is proposed for a wind system utilizing a DFIG generator. The system under consideration integrates three distinct control techniques: namely, sliding mode control, backstepping control, and fuzzy logic control. The integration of these techniques is intended to ensure the stability of the control and increase the robustness of the system, regardless of parametric and non-parametric variations.

The article is divided into five sections. In the preliminary section, the modelling of the doubly fed induction generator in the Park frame is presented, which is linked to the rotating field for its control. The objective is realised through the implementation of state formalism and a rotor power supply (two-level inverter). The integration of these components enables the implementation of control systems designed to regulate the power generated by the stator. The second section will present the methodology for developing a sliding mode control system to regulate the active and reactive power generated by the DFIG. The third section will be dedicated to the development of a backstepping control strategy for the system above. This will facilitate the convergence of errors towards zero and subsequent monitoring of active and reactive power rates.

Furthermore, it will ensure the stability and equilibrium of the system. In the final section, a hybrid sliding, backstepping and fuzzy control strategy of the DFIG will be presented and evaluated by numerous simulations in the MATLAB/Simulink environment. The objective of this study is twofold: firstly, to ascertain the interest of this novel approach, and secondly, to make comparisons with the results obtained in the preceding sections.

<sup>1,2,3,4</sup> LGE Research Laboratory, University of M'sila, M'sila 28000, Algeria.

E-mails: abdelghafour.herizi@univ-msila.dz, riyadh.rouabhi@univ-msila.dz, fayssal.ouaguenei@univ-msila.dz, abderrahim.zemmit@univ-msila.dz

## 2. MATHEMATICAL MODELING OF DFIG

The following matrix form describes the dynamic model of the doubly fed induction generator in the  $(d, q)$  reference frame, encompassing both electrical and mechanical dynamics [1, 20].

$$\dot{X} = AX + BU \quad (1)$$

where

$$X = [\varphi_{sd} \quad \varphi_{sq} \quad I_{rd} \quad I_{rq}]^T; U = [V_{sd} \quad V_{sq} \quad V_{rd} \quad V_{rq}]^T;$$

$$[A] = \begin{bmatrix} -\frac{1}{T_s} & \omega_s & \frac{M}{T_s} & 0 \\ -\omega_s & -\frac{1}{T_s} & 0 & \frac{M}{T_s} \\ \alpha & -\beta\omega & -\delta & (\omega_s - \omega) \\ \beta\omega & \alpha & -(\omega_s - \omega) & -\delta \end{bmatrix};$$

$$[B] = \begin{bmatrix} 1 & 0 & 0 & 0 \\ 0 & 1 & 0 & 0 \\ -\frac{M}{\sigma L_s L_r} & 0 & \frac{1}{\sigma L_r} & 0 \\ 0 & -\frac{M}{\sigma L_s L_r} & 0 & \frac{1}{\sigma L_r} \end{bmatrix}$$

with:

$$\sigma = 1 - \frac{M^2}{L_r L_s}; T_r = \frac{L_r}{R_r}; T_s = \frac{L_s}{R_s}; \alpha = \frac{M}{\sigma L_r L_s T_s}; \beta = \frac{M}{\sigma L_r L_s};$$

$$\delta = \frac{1}{\sigma} \left( \frac{1}{T_r} + \frac{M^2}{L_s T_s L_r} \right)$$

The equations for mechanics and electromagnetism are as follows:

$$J \frac{d\Omega}{dt} = C_{em} - C_r - f\Omega \quad (2)$$

$$C_{em} = P \frac{M}{L_s} (\varphi_{sq} I_{rd} - \varphi_{sd} I_{rq}) \quad (3)$$

In order to regulate the power production of the wind turbine, it is essential to have an objective control of the energetic and reactive powers. This can be achieved by establishing equations that connect the values of the rotor voltages to the energetic and reactive stator powers [21, 22].

By selecting a  $(d, q)$  reference frame associated with the rotating stator region and aligning the stator flux vector with the  $d$ -axis, the following results are obtained:  $\varphi_{sd} = \varphi_s$  and  $\varphi_{sq} = 0$ . Assuming a stable electric community and negligible stator resistance, the equation yields  $V_{sd} = 0$ ,  $V_{sq} = V_s$  and  $V_{sq} = V_s / \omega_s$ .

The above equations can be adapted to the simplifying assumptions as follows:

$$\begin{cases} I_{sd} = \frac{\varphi_s}{L_s} - \frac{M}{L_s} I_{rd} \\ I_{sq} = -\frac{M}{L_s} I_{rq} \end{cases} \quad (4)$$

$$\begin{cases} P_s = -\frac{M V_s}{L_s} I_{rq} \\ Q_s = \frac{V_s^2}{\omega_s L_s} - \frac{M V_s}{L_s} I_{rd} \end{cases} \quad (5)$$

$$\begin{cases} \varphi_{rd} = \left( L_r - \frac{M^2}{L_s} \right) I_{rd} + \frac{M V_s}{\omega_s L_s} \\ \varphi_{rq} = \left( L_r - \frac{M^2}{L_s} \right) I_{rq} \end{cases} \quad (6)$$

$$\begin{cases} V_{rd} = R_r I_{rd} + \left( L_r - \frac{M^2}{L_s} \right) \dot{I}_{rd} - g \omega_s \left( L_r - \frac{M^2}{L_s} \right) I_{rq} \\ V_{rq} = R_r I_{rq} + \left( L_r - \frac{M^2}{L_s} \right) \dot{I}_{rq} + g \omega_s \varphi_{rq} + g \frac{M V_s}{L_s} \end{cases} \quad (7)$$

The method used in electricity control involves disregarding coupling phrases and installing an impartial regulator on each axis. This enables independent control of both active and reactive power. This method is referred to as the direct approach, as the electricity regulators directly

control rotor voltages [8].

## 3. SLIDING MODE CONTROL

The primary concept of SMC is to confine the states of the machine within a predetermined region and then devise a control regulation that will consistently maintain the machine within that region [1, 10, 18]. SMC is comprised of three parts:

- Choice of switching surface: the sliding surface is determined by the trendy equation proposed by J.J. Slotine:

$$s(X) = \left( \frac{d}{dt} + \lambda \right)^{n-1} e \quad (8)$$

$$e = X^d - X$$

Where:

$\lambda$ : positive coefficient;  $e$ : error on the signal to be adjusted;  $n$ : system order.

- The convergence condition: is described using the Lyapunov equation [20], which ensures that the region is both attractive and invariant.

$$s(X) \dot{s}(X) < 0 \quad (9)$$

- Control calculation: the rules for the control set are described using the relation:

$$u = u^{eq} + u^n \quad (10)$$

where  $u^{eq}$  is the control vector that is equal and can be obtained by considering the sliding regime;  $u^n$ : represents the switching part of the control, which acts as a correction factor,  $u^n = k \text{sign}(s(X))$ .

### 3.1 ACTIVE POWER CONTROL

The sliding surface's expression is:

$$\begin{aligned} s(P) &= (I_{rq}^{ref} - I_{rq}) \\ \dot{s}(P) &= (\dot{I}_{rq}^{ref} - \dot{I}_{rq}) \end{aligned} \quad (11)$$

By substituting the expressions given in equations (5) and (7) for the current derivatives, we obtain:

$$\dot{s}(P) = \left( -\frac{L_s}{M V_s} \dot{P}_s^{ref} - \frac{V_{rq}}{L_r \sigma} - \frac{1}{L_r \sigma} \left( -R_r I_{rq} - g \omega_s L_r \sigma I_{rd} g \frac{M V_s}{L_s} \right) \right) \quad (12)$$

The control voltage  $V_{rq}$  is defined by:  $V_{rq} = V_{rq}^{eq} + V_{rq}^n$ , where  $s(P) = 0$ ,  $\dot{s}(P) = 0$  and  $V_{rq}^n = 0$ .

$$V_{rq}^{eq} = -\frac{L_s L_r \sigma}{M V_s} \dot{P}_s^{ref} + R_r I_{rq} + g \omega_s L_r \sigma I_{rd} + g \frac{M V_s}{L_s} \quad (13)$$

During the convergence mode,  $s(P) \dot{s}(P) < 0$  must be verified with:

$$V_{rq}^n = L_r \sigma k_1 \text{sign}(s(P)) \quad (14)$$

where  $k_1 > 0$ .

### 3.2 REACTIVE POWER CONTROL

The expression of the sliding surface becomes:

$$\begin{aligned} s(Q) &= (I_{rd}^{ref} - I_{rd}) \\ \dot{s}(Q) &= (\dot{I}_{rd}^{ref} - \dot{I}_{rd}) \end{aligned} \quad (15)$$

By replacing  $\dot{I}_{rd}^{ref}$  and  $\dot{I}_{rd}$  by their expressions given by equations (5) and (7), we obtain:

$$\dot{s}(Q) = \left( \left( \frac{V_s}{\omega_s M} - \frac{L_s}{V_s M} \dot{Q}_s^{ref} \right) - \frac{V_{rd}}{L_r \sigma} - \frac{1}{L_r \sigma} \left( -R_r I_{rd} + g \omega_s L_r \sigma I_{rq} \right) \right) \quad (16)$$

The control voltage  $V_{rd}$  is defined by:  $V_{rd} = V_{rd}^{eq} + V_{rd}^n$ .

$$V_{rd}^{eq} = L_r \sigma \left( \frac{V_s}{\omega_s M} - \frac{L_s}{V_s M} \dot{Q}_s^{ref} \right) + R_r I_{rd} - g \omega_s L_r \sigma I_{rq} \quad (17)$$

During the convergence mode, the condition  $s(Q)\dot{s}(Q) < 0$  must be verified with:

$$V_{rd}^n = L_r \sigma k_2 \text{sign}(s(Q)) \quad (18)$$

where  $k_2$  is a positive constant.

#### 4. BACKSTEPPING CONTROL

The structure and synthesis of the backstepping control will be presented in order to facilitate the development of an adequate algorithm that allows for the convergence of errors towards zero and the monitoring of the active and reactive power rates generated by a DFIG in a wind energy conversion system. This will subsequently guarantee the stability and equilibrium of the system.

The backstepping method is based on vector control, the control will be implemented in the point  $(d, q)$  taking into account the orientation of the following stator flux [12]:

$$\begin{cases} \varphi_{sd} = \varphi_s \\ \varphi_{sq} = 0 \end{cases} \quad (19)$$

In this part, we consider the new DFIG model in the frame  $(d, q)$  given by:

$$\begin{cases} V_{sd} = 0 \\ V_{sq} = \omega_s \varphi_s = V_s \\ V_{rd} = R_r I_{rd} + \frac{d\varphi_{rd}}{dt} - \omega_r \varphi_{rq} \\ V_{rq} = R_r I_{rq} + \frac{d\varphi_{rq}}{dt} + \omega_r \varphi_{rd} \end{cases} \quad (20)$$

Relationships between stator powers and rotor currents

$$\begin{cases} I_{rq}^{ref} = -\frac{L_s}{M V_s} P_s^{ref} \\ I_{rd}^{ref} = \frac{V_s}{M \omega_s} - \frac{L_s}{M V_s} Q_s^{ref} \end{cases} \quad (21)$$

Equations of the derivatives of reference rotor currents

$$\begin{cases} \dot{I}_{rq}^{ref} = -\frac{L_s}{M V_s} \dot{P}_s^{ref} \\ \dot{I}_{rd}^{ref} = -\frac{L_s}{M V_s} \dot{Q}_s^{ref} \end{cases} \quad (22)$$

Equations of rotor current derivatives

$$\begin{cases} \dot{I}_{rd}^{ref} = \frac{1}{\sigma L_r} (V_{rd} - R_r I_{rd} + g \omega_s L_r I_{rq} \sigma) \\ \dot{I}_{rq}^{ref} = \frac{1}{\sigma L_r} (V_{rq} - R_r I_{rq} - g \omega_s L_r I_{rd} \sigma - g \frac{M V_s}{L_s}) \end{cases} \quad (23)$$

The backstepping control consists in identifying the errors  $E_1$  and  $E_2$ , which respectively represent the error between the real stator active power  $P_s$  and the reference power  $P_s^{ref}$  which will be directly proportional to the rotor current of axis  $q$ , as well as the stator reactive power  $Q_s$  and the reference power  $Q_s^{ref}$  which will be proportional to the rotor current of axis  $d$ .

$$\begin{cases} E_1 = I_{rq}^{ref} - I_{rq} \\ E_2 = I_{rd}^{ref} - I_{rd} \end{cases} \quad (24)$$

The derivative of this error is given by:

$$\begin{cases} \dot{E}_1 = \dot{I}_{rq}^{ref} - \dot{I}_{rq} \\ \dot{E}_2 = \dot{I}_{rd}^{ref} - \dot{I}_{rd} \end{cases} \quad (25)$$

The first Lyapunov function is defined by:

$$V = \frac{1}{2} [E_1^2 + E_2^2] \quad (26)$$

To have the derivative of the Lyapunov function zero, we must choose the errors as follows:

$$\begin{cases} \dot{E}_1 = -K_1 E_1 \\ \dot{E}_2 = -K_2 E_2 \end{cases} \quad (27)$$

Subsequently, the derivative of the Lyapunov function

with respect to time is obtained as follows:

$$\dot{V} = -K_1 E_1^2 - K_2 E_2^2 \text{ with } K_1, K_2 > 0 \quad (28)$$

From equations (22), (23) and (25) the derivative of the errors  $E_1$  and  $E_2$  becomes:

$$\begin{cases} \dot{E}_1 = \frac{-L_s}{M V_s} \dot{P}_s^{ref} - \frac{1}{\sigma L_r} (V_{rq} - R_r I_{rq} - g \omega_s L_r I_{rd} \sigma - \frac{g M V_s}{L_s}) \\ \dot{E}_2 = \frac{-L_s}{M V_s} \dot{Q}_s^{ref} - \frac{1}{\sigma L_r} (V_{rd} - R_r I_{rd} + g \omega_s L_r I_{rq} \sigma) \end{cases} \quad (29)$$

According to equation (27), we find:

$$\begin{cases} -K_1 E_1 = \frac{-L_s}{M V_s} \dot{P}_s^{ref} - \frac{1}{\sigma L_r} (V_{rq} - R_r I_{rq} - g \omega_s L_r I_{rd} \sigma - \frac{g M V_s}{L_s}) \\ -K_2 E_2 = \frac{-L_s}{M V_s} \dot{Q}_s^{ref} - \frac{1}{\sigma L_r} (V_{rd} - R_r I_{rd} + g \omega_s L_r I_{rq} \sigma) \end{cases} \quad (30)$$

So the control will be:

$$\begin{cases} V_{rq} = \sigma L_r \left( \frac{-L_s}{M V_s} \dot{P}_s^{ref} + K_1 E_1 \right) + R_r I_{rq} + g \omega_s L_r I_{rd} \sigma + \frac{g M V_s}{L_s} \\ V_{rd} = \sigma L_r \left( \frac{-L_s}{M V_s} \dot{Q}_s^{ref} + K_2 E_2 \right) + R_r I_{rd} - g \omega_s L_r I_{rq} \sigma \end{cases} \quad (31)$$

#### 5. HYBRID SLIDING MODE-BACKSTEPPING CONTROL AND FUZZY LOGIC

The principal disadvantage of sliding mode control (SMC) is the elevated switching frequency, which is known as 'chattering'. It is inadvisable to employ chattering, as it has the potential to induce unmodeled high-frequency modes within the controlled system. In order to solve this problem, it is essential to have a control that will predict the performance even if the system model is not well known [1, 2, 12].

In the following, we put the concept of backstepping sliding mode hybrid control into practice at DFIG. Then, we combined this hybrid control by fuzzy logic. Our aim is to prove that hybrid control is a robust control and can solve the drawbacks of sliding mode control effectively.

##### 5.1 HWYBRID SLIDING MODE-BACKSTEPPING CONTROL STRATEGY FOR A DFIG

The hybrid sliding mode-backstepping control method is initially presented with the objective of simultaneously ensuring the stability and robustness of the system. The backstepping and sliding mode techniques are two methods that utilize the concept of a Lyapunov function. This common ground will be employed to develop a novel control strategy that integrates the two techniques. Indeed, the two criteria that permit the system dynamics to converge towards the sliding surface are:

$$\begin{cases} s(x)\dot{s}(x) < 0 \\ \dot{V}(x) < 0 \end{cases} \quad (32)$$

The hybrid control is based on a modification of the sliding mode controller, whereby the value of the equivalent control is maintained and the attractive control is replaced with the backstepping control (Fig. 1).

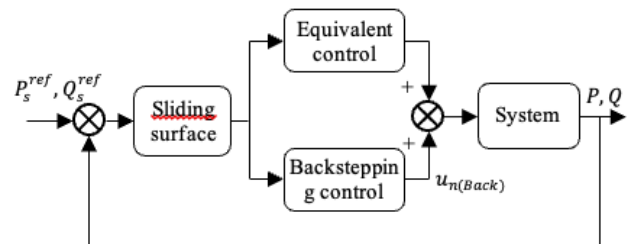


Fig. 1 – Structure of the hybrid sliding-backstepping controller.

Therefore, the combination of the two elements ensures the stability and robustness of the system under investigation.

$$u_{hybrid} = u_{eq(SMC)} + u_{n(Back)} \quad (33)$$

where  $u_{eq(SMC)}$  is the generated by sliding mode control and  $u_{n(Back)}$  is the generated by backstepping control.

The global equation of the  $V_{rq}$  and  $V_{rd}$  controls takes the following forms:

$$\begin{cases} V_{rq}^{eq} = -\frac{\sigma L_s L_r}{MV_s} \dot{P}_s^{ref} + R_r I_{rq} + g \omega_s \sigma L_r I_{rd} + g \frac{MV_s}{L_s} \\ V_{rq}^n = \sigma L_r \left( -\frac{L_s}{MV_s} \dot{P}_s^{ref} + K_1 E_1 \right) + R_r I_{rq} + g \omega_s \sigma L_r I_{rd} + \frac{g MV_s}{L_s} \end{cases} \quad (34)$$

$$\begin{cases} V_{rd}^{eq} = \sigma L_r \left( \frac{V_s}{M \omega_s} - \frac{L_s}{MV_s} \dot{Q}_s^{ref} \right) + R_r I_{rd} - g \omega_s \sigma L_r I_{rq} \\ V_{rd}^n = \sigma L_r \left( -\frac{L_s}{MV_s} \dot{Q}_s^{ref} + K_2 E_2 \right) + R_r I_{rd} - g \omega_s \sigma L_r I_{rq} \end{cases} \quad (35)$$

A schematic diagram of the hybrid sliding mode-backstepping control of the DFIG is provided in Fig. 2. It consists of two discrete functionalities. The first is the equivalent function generated by the SMC, and the second is the switching function generated by the backstepping control.

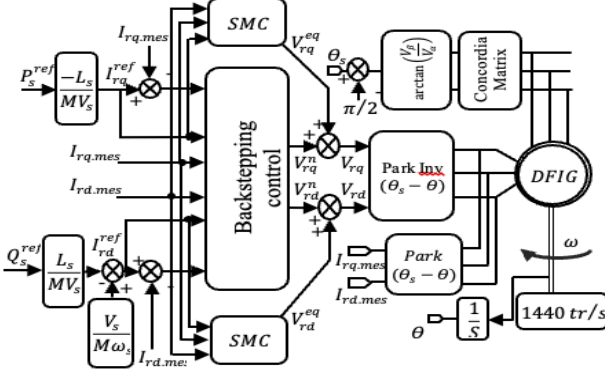


Fig. 2 – Block diagram of the structure of the Hybrid Sliding-Backstepping control.

## 5.2 FUZZY HYBRID CONTROL

This work presents the implementation of a hybrid control strategy combining sliding mode, backstepping, and fuzzy logic controllers for regulating active and reactive power in a DFIG-based wind energy system. This technique entails substituting the gains of the backstepping control regulations with a type 1 fuzzy controller, which employs a single input, namely the discrepancy between the measured value and the reference value.

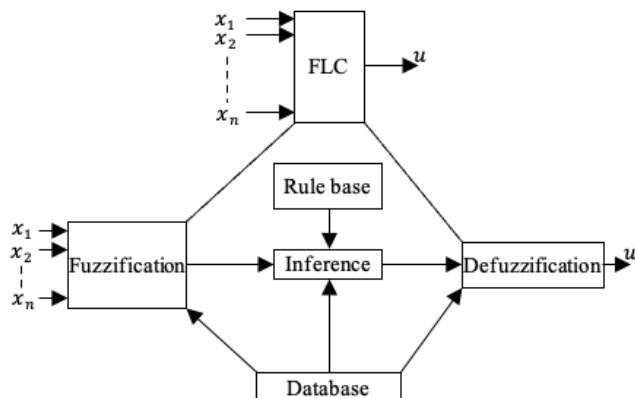


Fig. 3 – Description of the structure of a fuzzy logic controller.

This approach permits the identification of the constituent elements of the generator supply voltages, thereby ensuring comprehensive stability in accordance with the tenets of Lyapunov theory. This is accomplished by maintaining stable dynamics at each instance when the discrepancies between the reference and actual quantities are at their minimum.

Figure 3 illustrates the structure of a fuzzy logic controller, as described in reference [23].

The following section presents a proposal for replacing the existing active and reactive power regulators with a sliding, backstepping, and fuzzy mode regulator. The objective of this proposal is to achieve robust, high-performance regulation. It is proposed that an equivalent control part (SMC) and a second switching function generated by backstepping control and fuzzy logic at one input be employed as a means of regulating the error between the measured value and its reference, as illustrated in Fig. 4. This is accomplished through the utilization of

$$u_{n(Back)} = u_{Back} + u_{Fuzzy} \quad (36)$$

The global equation of the  $V_{rq}$  and  $V_{rd}$  controls takes the following forms:

$$\begin{cases} V_{rq}^{eq} = -\frac{\sigma L_s L_r}{MV_s} \dot{P}_s^{ref} + R_r I_{rq} + g \omega_s \sigma L_r I_{rd} + g \frac{MV_s}{L_s} \\ V_{rq}^{Back} = -\frac{\sigma L_r L_s}{MV_s} \dot{P}_s^{ref} + R_r I_{rq} + g \omega_s \sigma L_r I_{rd} + \frac{g MV_s}{L_s} \\ V_{rq}^{Fuzzy} = \sigma L_r (K_1 E_1) \end{cases} \quad (37)$$

$$\begin{cases} V_{rd}^{eq} = \sigma L_r \left( \frac{V_s}{M \omega_s} - \frac{L_s}{MV_s} \dot{Q}_s^{ref} \right) + R_r I_{rd} - g \omega_s \sigma L_r I_{rq} \\ V_{rd}^{Back} = \sigma L_r \left( -\frac{L_s}{MV_s} \dot{Q}_s^{ref} \right) + R_r I_{rd} - g \omega_s \sigma L_r I_{rq} \\ V_{rd}^{Fuzzy} = \sigma L_r (K_2 E_2) \end{cases} \quad (38)$$

The fuzzy controller developed in this work is by the following figure:

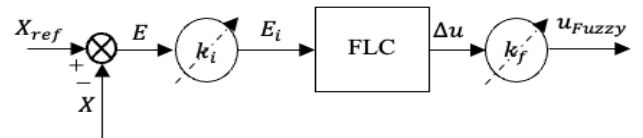


Fig. 4 – Diagram illustrates the configuration of a fuzzy controller.

In the figure above, the proposed fuzzy controller is composed by: A normalization factor  $k_i$  associated with the error ( $e$ ) and  $k_f$  associated with the variation of the control  $\Delta u$ , fuzzification block of the error, fuzzy control rules, decide the control gains  $k_i$  according to the current operating state of the controlled system and a defuzzification block used to convert the fuzzy control variation to a digital value.

In the proposed controller (fuzzy logic system of the Mamdani type), we note that it is important to choose the values of  $k_i$  and  $k_f$ . When combined with an appropriate distribution, a suitable option has the potential to facilitate a successful conception, provided that the distribution is appropriate. Conversely, an inappropriate selection may necessitate the implementation of lengthy corrective measures in subsequent phases. In certain cases, it may be necessary to redefine the ranges of values in order to circumvent failure in the design. A well-informed decision requires a certain degree of expertise and familiarity with the system in question. The

formulation of fuzzy rules is illustrated in Table 1, as referenced in [23].

Table 1

The basis rules of the fuzzy logic controller.

Input	Negative Big	Negative Medium	Zero	Positive Medium	Positive Big
Output	Positive Big	Positive Medium	Zero	Negative Medium	Negative Big

The membership functions for input and output are illustrated in Figs. 5 and 6, respectively.

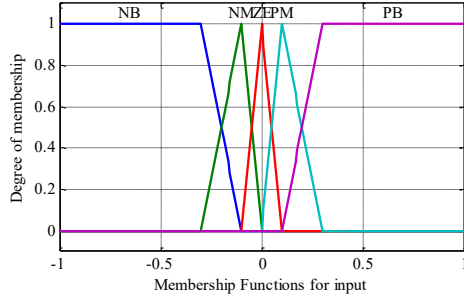


Fig. 5 – Membership functions of input ( $E$ ).

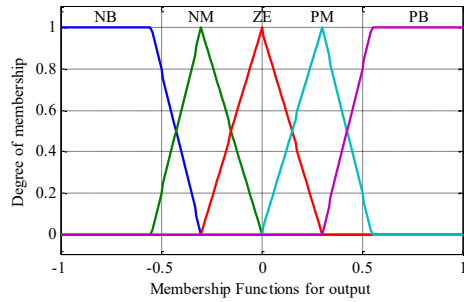


Fig. 6 – Membership functions of output ( $u_{Fuzzy}$ ).

## 6. RESULTS OBTAINED

In this section, we have presented the active and reactive power curves in a manner that demonstrates the efficacy and resilience of the proposed control methodology.

Parameters of the DFIG are equal:

$P_n = 4 \text{ KW}$ ,  $I_n = 15/8.6 \text{ A}$ ,  $\Omega_n = 1440 \text{ rpm}$ ,  $P = 2$ ,  $R_s = 1.2 \Omega$ ,  $R_r = 1.8 \Omega$ ,  $L_s = 0.1554 \text{ H}$ ,  $L_r = 0.1568 \text{ H}$ ,  $M = 0.15 \text{ H}$ ,  $J = 0.2 \text{ Kg.m}^2$ ,  $f = 0.001 \text{ IS}$ .

The simulation results are illustrated in the following figures:

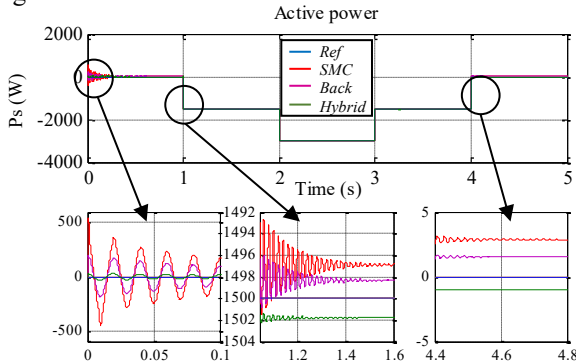


Fig. 7 – Active power produced for the three controls.

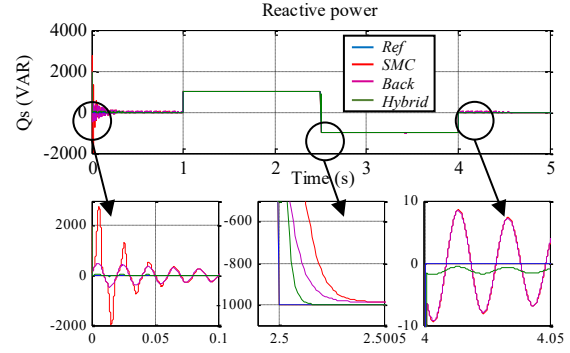


Fig. 8 – Reactive power produced for the three controls.

The results presented herein illustrate the shape of both active and reactive powers over the course of a five-second simulation. The three synthesised controls demonstrate robust performance and are effective in achieving the desired outcomes. Nevertheless, the hybrid sliding-backstepping and fuzzy mode control strategy appears to be the optimal control strategy, exhibiting near-smooth power shapes and precise tracking of the setpoint shapes.

The discrepancy between the simulation outcomes yielded by the various control methodologies implemented on our system can be quantified through four criteria: the integral of the squared error (ISE), the integral of the absolute value of the error (IAE), the integral of the time multiplied by the absolute value of the error (ITAE), and the integral of the time multiplied by the squared error (ITSE). The performance criteria are defined in mathematical terms as follows:

- The integral of the squared error is defined as follows:

$$ISE = \int_0^T e^2(t) dt \quad (39)$$

- The integral of the absolute value of the error is given by:

$$IAE = \int_0^T |e(t)| dt \quad (40)$$

- The integral of time, multiplied by the absolute value of the error, is given by the following equation:

$$ITAE = \int_0^T t \cdot |e(t)| dt \quad (41)$$

- The integral of time multiplied by the squared error:

$$ITSE = \int_0^T t \cdot e^2(t) dt \quad (42)$$

Table 2

Comparative study of the controls developed for the DFIG

		Controls developed for our system		
		Criteria	SMC	Backstepping Control
Active power	IAE	44.8727	23.9328	11.0086
	ISE	$5.0822 \times 10^3$	$1.3902 \times 10^3$	244.7824
	ITAE	42.7307	22.8551	22.0190
	ITSE	894.4104	309.5213	519.7187
Reactive power	IAE	64.6596	46.9782	8.0207
	ISE	$4.6134 \times 10^4$	$8.9186 \times 10^3$	232.8273
	ITAE	16.9647	16.3321	15.7186
	ITSE	$1.4998 \times 10^3$	848.5322	340.1512
Settling time (s)		0.653	0.6322	0.002542

The results presented in the table above clearly show that the values of the proposed hybrid control is the most robust control compared to other techniques.

## 7. CONCLUSION

In order to enhance the functionality of the control

system, this study introduces a hybrid approach integrating backstepping with sliding mode control and fuzzy logic.

The objective of this paper is to present a comparative analysis of the diverse control techniques employed on the aforementioned system, with a particular emphasis on the doubly-fed induction generator. In order to achieve this, two fundamental qualitative and quantitative approaches were employed. The results clearly demonstrate that the proposed hybrid control represents the most efficient and effective approach for the wind energy conversion system under consideration, in comparison to the other control techniques.

#### ACKNOWLEDGMENTS

The author wishes to express their gratitude to the research team at the Electrical Engineering Laboratory at M'sila University for their guidance and ongoing support.

#### CREDIT AUTHORSHIP CONTRIBUTION STATEMENT

Abdelghafour Herizi: conceptualization, methodology, programming, writing – original draft, validation.  
Riyadh Rouabhi: investigation, writing – review & editing.  
Fayssal Ouagueni: supervision, resources, results curation.  
Abderrahim Zemmit: formal analysis, visualization, writing – review & editing.

Received on 24 September 2024.

#### REFERENCES

1. R. Rouabhi, A. Herizi, A. Djeriou, *Performance of robust type-2 fuzzy sliding mode control compared to various conventional controls of doubly-fed induction generator for wind power conversion systems*, *Energies*, **17**, 3778, pp. 1–25 (2024).
2. E. Farah, Y. Ihedrane, B. Bossouf, M. Bouderbala, S. Motahhir, M. Masud, S. Aljahdali, M. El Ghamrasni, *Robust sliding Backstepping mode control of a wind system based on the DFIG generator*, *Scientific Reports*, **12**, 11782, pp. 1–16 (2022).
3. S. Kouadria, E. Berkouk, Y. Messlem, M. Denai, *Improved control strategy of DFIG-based wind turbines using direct torque and direct power control techniques*, *Journal of Renewable and Sustainable Energy*, **10**, 4, pp. 1–21, (2018).
4. C.R. Raghavendran, J.P. Roselyn, D. Devaraj, *Development and performance analysis of intelligent fault ride through controls chemin the dynamic behaviour of grid connected DFIG based wind systems*, *Energy Reports*, **6**, pp. 2560–2576 (2020).
5. B. Desalegn, D. Gebeyehu, B. Tamrat, *Wind energy conversion technologies and engineering approaches to enhancing wind power generation*, *Heliyon*, **8**, pp. 1–21 (2022).
6. Y. Sahri, S. Tamalouzt, S.L. Belaid, M. Bajaj, S.S. Ghoneim, H.M. Zawbaa, S. Kamel, *Performance improvement of Hybrid System-based DFIG-Wind/PV/Batteries connected to DC and AC grid by applying Intelligent Control*, *Energy Reports*, **9**, pp. 2027–2043 (2023).
7. R. Rouabhi, A. Herizi, S. Djeriou, A. Zemmit, *Hybrid type-1 and 2 fuzzy sliding mode control of the induction motor*, *Revue Roumaine des Sciences Techniques, Série Électrotechnique et Énergétique*, **69**, 2, pp. 147–152 (2024).
8. C. Hamid, A. Derouich, M. Taoussi, O. Zamzoum, A. Hanafi, *An improved performance variable speed wind turbine driving a doubly fed induction generator using sliding mode strategy*, *IEEE 2nd International Conference on Electronics, Control, Optimization and Computer Science (ICECOCS)*, Kenitra, Morocco, (2020).
9. B. Kelkoul, A. Boumediene, *Stability analysis and study between classical sliding mode control (SMC) and super twisting algorithm (STA) for doubly fed induction generator (DFIG) under wind turbine*, *Energy*, **214** (2021).
10. A. Herizi, R. Rouabhi, A. Zemmit, *Comparative study of the performance of a sliding, sliding-fuzzy type 1 and a sliding-fuzzy type 2 control of a permanent magnet synchronous machine*, *Przegląd Elektrotechniczny*, **98**, 11, pp. 21–29 (2022).
11. A. Ghalem, A. Naceri, Y. Djeriri, *Backstepping control of a wind energy conversion system based on a DFIG connected to the grid*, *Przegląd Elektrotechniczny*, **99**, 12, pp. 98–103 (2023).
12. A. Herizi, R. Rouabhi, A. Zemmit, *Speed control of doubly fed induction motor using backstepping control with interval type-2 fuzzy controller*, *Diagnostyka*, **24**, 3, pp. 1–8 (2023).
13. A. Herizi, A. Benyounes, R. Rouabhi, A. boudras, F. Ouagueni, A. Zemmit, *Robust fuzzy – backstepping mode control of an induction motor*, *Studies in Engineering and Exact Sciences*, **5**, 1, pp. 1317–1334 (2024).
14. A. Benyounes, A. Herizi, M. Zegait, M. Bouras, B. Nail, I.E. Tibermacine, *Fuzzy backstepping control for enhanced stability of a quadrotor unmanned aerial vehicle*, *Studies in Engineering and Exact Sciences*, **5**, 1, pp. 746–769 (2024).
15. C. Dualibe, M. Verleysen, P.G.A. Jespers, *Design of analog fuzzy logic controllers in CMOS technologies*, Kluwer Academic Publishers, New York (2003).
16. R. Lowen, A. Verschoren, *Foundations of generic optimization, Volume 2: applications of fuzzy control, genetic algorithms and neural networks*, Springer (2008).
17. M. Errouha, A. Derouich et al., *Optimization and control of water pumping PV systems using fuzzy logic controller*, *Energy Reports*, **5**, pp. 853–865 (2019).
18. M.S. Adouairi, B. Bossoufi, S. Motahhir, I. Saady, *Application of fuzzy sliding mode control on a single-stage grid-connected PV system based on the voltage-oriented control strategy*, *Results in Engineering*, **17**, pp. 1–9 (2023).
19. A.J.G. Malar, C.A. Kumar, A.G. Saravanan, *IoT based sustainable wind green energy for smart cities using fuzzy logic based fractional order darwinian particles warm optimization*, *Measurement*, **166** (2020).
20. A. Herizi, A. Zemmit, R. Rouabhi, F. Ouagueni, *New design of robust controller based on fuzzy 12 linguistic variables for wind power conversion system*, *Przegląd Elektrotechniczny*, **100**, 10, pp. 89–92 (2024).
21. H.H.H. Mousa, A. Youssef, E.E.M. Mohamed, *Hybrid and adaptive sectors P&O MPPT algorithm based wind generation system*, *Renewable Energy*, **145**, pp. 1412–1429 (2020).
22. M. Ahmad Soomro, Z. Ahmad Memon, M. Kumar, M. Hussain Baloch, *Wind energy integration: Dynamic modeling and control of DFIG based on super twisting fractional order terminal sliding mode controller*, *Energy Reports*, **7**, pp. 6031–6043 (2021).
23. A. Herizi, R. Rouabhi, S. Krim, E. Hachi, *Hybrid control using fuzzy sliding mode control of doubly fed induction machine*, *1<sup>st</sup> International Conference on Electronics, Artificial Intelligence and New Technologies*, Oum El Bouaghi, Algeria (2021).